Tellus (2007), 59B, 577–586
Printed in Singapore. All rights reserved

TELLUS

Sensitivity of Lagrangian Stochastic footprints to turbulence statistics

By M. GÖCKEDE[1]*, C. THOMAS[1], T. MARKKANEN[2], M. MAUDER[3], J. RUPPERT[2] and T. FOKEN[2], [1]*Department of Forest Science, Oregon State University, Corvallis, OR, 97331, USA;* [2]*Department of Micrometeorology, University of Bayreuth, D-95440 Bayreuth, Germany;* [3]*Agriculture and Agri-Food Canada, Research Branch, Ottawa, ON, Canada, K1A 0C6*

(Manuscript received 28 April 2006; in final form 11 January 2007)

ABSTRACT

This study tests the sensitivity of a Lagrangian Stochastic footprint model to the turbulence statistics describing the flow field, with a focus on the within canopy processes. Representative profiles of the input velocity statistics are taken from a long-term dataset of turbulence measurements within and above a tall spruce canopy. Based on a wavelet tool, which allows a detailed analysis of coherent structures along the vertical profile, we characterize several typical states of coupling and decoupling between surface, canopy and atmosphere. For each coupling regime, three flux footprints using different sources for turbulence statistics are compared: the first based on conditionally-averaged measurements, the second on a simple numerical solution and the third on measurements taken from literature. The effects of profile smoothing and connecting measured canopy data to parametrized atmospheric surface layer profiles are considered. Significant differences between footprints based on modelled and measured profiles were found for exchange regimes with the lower section of the profiles decoupled from the atmospheric surface layer. As such cases are likely to occur for tall canopies with moderate density, our results suggest that the accuracy of Lagrangian Stochastic footprint modelling could be improved by using better turbulence profiles for different exchange regimes.

1. Introduction

Sites for flux towers, such as those represented by FLUXNET (e.g. Baldocchi et al., 2001) are chosen according to their ecological importance, accessibility, or access to infrastructure; thus, micrometeorological aspects often play only a minor role for the site selection. As a result, sites are often located in topographically complex terrain, or fetches over the target land-use type are short due to a heterogeneous land cover structure, i.e. conditions that may compromise the collection of high quality meteorological data sets (e.g. Rebmann et al., 2005). The application of the eddy-covariance technique, which is commonly used for the determination of exchange fluxes between surface and atmosphere (e.g. Aubinet et al., 2000; Baldocchi et al., 2000), requires a site dependent quality control to allow for a robust interpretation of the measurements (Foken et al., 2004). A key component in the data quality protocol is a footprint analysis that determines the spatial context of a measurement by defining a transfer function between sources or sinks of the signal and the sensor position (e.g. Schmid, 2002). The derived source area is crucial for the interpretation of micrometeorological data sets as it allows determining fetch requirements under changing atmospheric stability regimes, or assessing the influence of flow distortion caused by the terrain on the measurements (e.g. Göckede et al., 2004; Rebmann et al., 2005; Göckede et al., 2006).

A powerful tool to model source areas over forest is the Lagrangian Stochastic (hereafter referred to as LS) footprint model (e.g. Baldocchi, 1997; Rannik et al., 2000; Kljun et al., 2002; Rannik et al., 2003). This technique allows the consideration of effects of canopy flow on the measured fluxes, and a more realistic treatment of diffusion than the simpler analytic footprint models. Lagrangian stochastic models require characteristics of prevailing turbulence as input, such as the profiles of the mean wind speed $\overline{u}$, the velocity standard deviations (σ_u; σ_v; σ_w), or the dissipation rate of turbulent kinetic energy ϵ. As only very few generally valid characteristics of turbulence are known in the canopy space (e.g. Lee, 1998; Finnigan, 2000), these parameters often have to be approximated with crude generalizations and certain ad hoc assumptions for the canopy part of the model domain (Schmid, 2002).

In this study, we test the sensitivity of a footprint model (Rannik et al., 2000 2003) that builds on the Thomson (1987) forward LS trajectory model for particle dispersion to the input parameters specifying the turbulent flow field. A special focus

*Corresponding author.
e-mail: mathias.goeckede@oregonstate.edu
DOI: 10.1111/j.1600-0889.2007.00275.x

will be placed on within canopy flow processes and the role of the roughness sublayer (RSL), the layer extending from just above the canopy top to a level about twice the canopy height (e.g. Garratt, 1980; Leuning, 2000; Arya, 2001). A dataset of long-term measurements, for which all recommended procedures for quality assurance and quality control (Foken et al., 2004) were closely followed, serves as the reference to describe turbulent exchange processes within and above a tall spruce canopy. Representative profiles of input velocity statistics required for footprint modelling are derived by applying different filters to the collected data set. This filter deploys spectral wavelet analysis (Thomas and Foken, 2005) to detect and extract individual coherent structures in turbulent flow variables observed across a vertical profile of sonic anemometers. Based on this analysis, typical exchange regimes are determined to characterize the degree of coupling between the ground surface, the canopy and the atmosphere (Thomas and Foken, 2007).

Assuming these measured, conditionally-averaged flow statistics constitute the most accurate way to describe canopy turbulence, this study assesses the uncertainty introduced to footprint modelling by using flow statistics that are commonly available to footprint modellers when no in-situ profile of turbulence were available. For the latter case, two simple methods are applied to describe the canopy flow regime. First, we use a model approach, the one-and-a-half order closure model by Massman and Weil (1999), to parametrize the profiles of the flow statistics based on local canopy architecture. Second, we use measured profiles available from literature (here: Rannik et al., 2003), which represent a different type of ecosystem. The impact of applying different descriptions of the canopy flow is tested by comparing the dimension and the position of source areas.

2. Data sources

For all sources of profile data described in this section, heights were normalized with the mean canopy height, h_c, to compensate for different canopy heights at different sites.

2.1. The WALDATEM-2003 dataset

A long-term data set of turbulence measurements collected during the WALDATEM-2003 (WAveLet Detection and Atmospheric TurbulencE Measurements, see Thomas et al., 2004) experiment within and above a tall spruce canopy was used to extract turbulence statistics required to describe the model domain for the footprint model. This experiment was conducted at the Waldstein Weidenbrunnen FLUXNET site (Gerstberger et al., 2004) operated by the University of Bayreuth, Germany. The site is located in the Fichtelgebirge mountains in Northeastern Bavaria (50 °09′ N, 11 °52′ E, 775 m a.s.l.). The terrain in the vicinity of the tower is hilly with slopes of moderate steepness, and is mainly covered by spruce forest with a mean canopy height (h_c) of 19 m around the tower. The entire experiment was

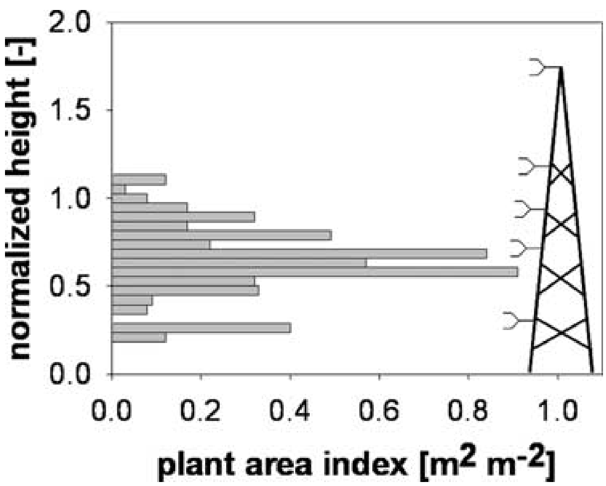

Fig. 1. Vertical profile of the plant area index (PAI) measured at the Waldstein Weidenbrunnen site. The total plant area index is 5.2 [m^2 m^{-2}] (Thomas and Foken, 2007). The tower indicates the positions of the five sonic anemometers. Heights were normalized by the mean canopy height 19 m.

conducted from April 28 to August 03, 2003; however, for this study we used only data collected between June 24 and July 17.

The WALDATEM dataset includes a profile of five sonic anemometers, installed at 5.5 m, 13.6 m, 17.7 m, 22.4 m, and 33 m above ground level. Fig. 1 shows the normalized measurements heights, and the profile of the plant area index (PAI) measured at the Waldstein Weidenbrunnen site (Thomas and Foken, 2007).

The sonic anemometers provided high-frequency time series of turbulent variables; their data were used to compute the turbulent exchange. Details of the experimental set up can be found in Thomas and Foken (2006).

2.2. *Profile data by Rannik et al. (2003)*

Rannik et al. (2003) used observations of wind statistics within and above a Northern Scots pine forest to drive their forward LS footprint model, which takes into account the effect of diabatic stratification on the footprint predictions. Their profiles are based on measurements at the Hyytiälä site, which is located in southern Finland (61 °51′ N, 24 °17’ E, 181 m a.s.l.), with a mean canopy height of 14 m close to the tower. Measurement levels used to derive the profiles of the flow statistics were 2.0 m, 9.5 m, 23.3 m, and 46 m. The profiles used within the context of this study are shown in Fig. 2. Please refer to Rannik et al. (2003) for details on instrumentation and profile parametrization.

2.3. *One-and-a-half order closure model by Massman and Weil (1999)*

The one-and-a-half order closure model by Massman and Weil (1999) predicts the vertical profiles of turbulence statistics (i.e. σ_u, σ_v and σ_w) inside the forest canopy under neutral

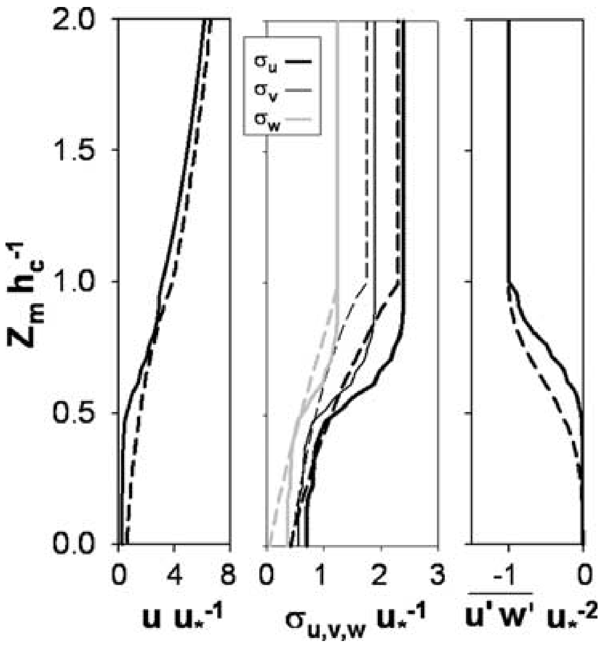

Fig. 2. Profiles of the flow statistics taken from the alternative data sources described in Sections 2.2 and 2.3. All data shown are examples for neutral stability of atmospheric stratification. Solid lines: Profiles derived with the Massman and Weil (1999) model, based on PAI profiles measured at the Waldstein Weidenbrunnen site; dashed lines: measurements from a Scots pine forest, published by Rannik et al. (2003). The profiles measured at the Waldstein Weidenbrunnen site itself are shown in more detail in Figure 5. Z_m: measurement height [m]; h_c: canopy height [m]; $\overline{u}$: Horizontal wind speed [m s^{-1}]; u*: Friction velocity at the measurement height [m s^{-1}]; $\sigma_{u,v,w}$: Standard deviations of alongwind (u), crosswind (v) and vertical wind (w) component [m s^{-1}]; $\overline{u'w'}$: vertical momentum flux [m^2 s^{-2}].

stratification according to the plant area distribution at a site. It builds on an analytical one-dimensional model of momentum transfer by Massman (1997) to predict the profiles of the vertical momentum flux ($\overline{u'w'}$) and mean wind speed ($\overline{u}$). In addition to the plant area distribution, the model requires the leaf drag coefficient C_d and the foliage-sheltering factor P_m in determining the profiles of the flow statistics. We used constant values of $C_d = 0.2$ and $P_m = 2$ for these parameters, with P_m having the inverse value of the clumping index of 0.5, which is appropriate for coniferous species (e.g. Marcolla et al., 2003).

Representative profiles for the Waldstein Weidenbrunnen site were computed using the PAI profile shown in Fig. 1. The normalized profiles derived by this additional data source are shown in Fig. 2.

3. Lagrangian Stochastic footprint modelling

Lagrangian stochastic footprint approaches assume that the dispersion of a passive scalar in turbulent flow can be described by tracking the trajectories of a finite number of independent particles on their passage through the model domain (e.g. Sawford, 1985; Leclerc and Thurtell, 1990). The performance of any LS model is therefore based on the definition of the flow field within this model domain, which is described by the imposed profiles of turbulence statistics.

In contrast to the Eulerian analytical footprint models (e.g. Schuepp et al., 1990; Horst and Weil, 1992; Schmid, 1997), LS models allow to distinguish between several vertical layers, each of which may have individual flow statistics (Baldocchi, 1997; Rannik et al., 2000 2003). The applicability of LS footprint models is not restricted to the atmospheric surface layer as is the case for analytical models, and an arbitrary vertical distribution of sources for the quantity to observe can be implemented. To apply LS models for footprint prediction, stationarity of the turbulent flow field is demanded as a basic requirement, and all models operated in forward mode are based on the inverted plume assumption (e.g. Schmid and Oke, 1988; Schmid, 2002) and are thus restricted to horizontally homogeneous flow conditions.

In this study, we used the Thomson (1987) three-dimensional forward LS trajectory model of Langevin type (e.g. Wilson et al., 1983; Wilson and Sawford, 1996) that assumes turbulence statistics to be Gaussian. The footprint calculation and the exact formulation of the parametrizations above the roughness sublayer, including the effect of stability on the profiles, is proposed by Rannik et al. (2003). In this approach, in addition to being carried downwind by horizontal advection, the particles are dispersed by turbulent diffusion in vertical, mean alongwind and mean crosswind directions. The particles tending downwards near to the surface are perfectly reflected at the height z_r. The required input data are profiles of the mean wind speed $\overline{u}$, the velocity standard deviations (σ_u; σ_v; σ_w), and the vertical momentum flux $\overline{u'w'}$. In addition, the dissipation rate of the turbulent kinetic energy, ϵ, is internally parametrized as a function of atmospheric stability, while the Lagrangian structure function constant, C_0, is set to a constant value of 4 (Rannik et al., 2003). The input parameters can either be measured, or parametrized with closure models, such as proposed by Massman and Weil (1999), and the effect of stability on the profiles can be accounted for (Rannik et al., 2003). Furthermore, atmospheric stability (using the Obukhov length, L, at the highest measurement level), surface roughness length z_0, and receptor height z_m need to be specified. A receptor height of 33.05 m was used, which corresponds to the uppermost measurement level at the Waldstein tower. For this study, the simulations are performed releasing particles from a height equal to 0.005 times the canopy height, which was also the height of perfect reflection (z_r), and tracked until an upwind distance accounting for approximately 90% of the total flux. To examine the influence of source heights on the footprints, additional runs were performed with particle release from the heights of 0.5 and 0.9 times the canopy height.

4. Analysis of coherent structures

The determination of exchange regimes was based on the analysis of coherent structures at different observation heights.

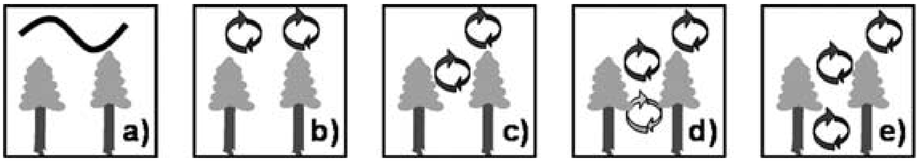

Fig. 3. Exchange regimes determined with the wavelet tool, indicating how deep coherent structures penetrate into the canopy according to the volume of the canopy that is coupled with the atmosphere. a) Waves (W); b) Decoupled canopy (Dc); c) Decoupled subcanopy (Ds); d) Partly coupled subcanopy (Cs); e) Fully coupled canopy (C).

Coherent structures were extracted from the sampled time series using the wavelet transform by a method described in Thomas and Foken (2005). Characteristic time scales of coherent structures were computed from the spectral peak in the wavelet variance spectrum for each averaging interval and for each variable separately. The characteristic time scale was then used to detect individual coherent structures in each 30-min interval individually.

The relative contribution of coherent structures to the total flux was determined by conditionally sampling the detected coherent structures (Thomas and Foken, 2007). This method uses a triple decomposition (Antonia et al., 1987) of a turbulent variable into a high-frequency part, a part attributed to the occurrence of coherent structures, and a mean part to partition fluxes attributed to different eddy sizes.

4.1. Exchange regimes determined with the wavelet tool

The contribution of coherent structures to the vertical flux of sensible heat was used to observe coherent structures in the vertical profile of sonic anemometers as described in Thomas and Foken (2007). As a result, it was determined how deep coherent structures penetrate into the canopy and which volume of the canopy participates in the mixing. In the following, we will refer to 'subcanopy' as the trunk space ($0 \leq z\, h_c^{-1} \leq 0.4$ see Fig. 1), and to 'canopy' as the crown space ($0.4 < z\, h_c^{-1} \leq 1.2$). We differentiated five exchange regimes (Fig. 3) for the WALDATEM-2003 dataset:

Wave motion (W). The flow above the canopy is dominated by wave motion rather than by turbulence (Fig. 3a). These periods can be detected by analyzing the phase angle in the cross-spectrum between velocity and scalar variables. We assume the atmosphere to be decoupled from the canopy and subcanopy spaces and thus the exchange of energy and matter to be negligible.

Decoupled canopy (Dc). The atmospheric layer above the canopy is mixed, but nevertheless is decoupled from the canopy and subcanopy layers (Fig. 3b). The direction of the fluxes contributed by the sweep and ejection phases of coherent structures are opposite to those in the overlying atmosphere. In general, there is no transfer of energy and matter into or out of the canopy.

Decoupled subcanopy (Ds). The atmosphere is coupled with the canopy but decoupled from the subcanopy space (Fig. 3c). The volume, of that participates in the exchange is limited to the canopy layer. The flux contribution of the sweep and ejection phases of coherent structures at the 'bottleneck' of the canopy indicates either fluxes opposite in sign or negligible flux fractions in relation to the canopy top and the overlying atmosphere.

Partly coupled subcanopy (Cs). The exchange between the atmosphere and the subcanopy is forced by the strong sweep motion of coherent structures only (Fig. 3d). The ejection phases either do not contribute significantly to the transport or have fluxes opposite in sign in relation to the canopy top and the atmosphere. This exchange regime is a transition regime between Ds and C.

Fully coupled canopy (C). The atmosphere, the canopy and the subcanopy spaces are in a fully coupled state (Fig. 3e). Both ejection and sweep phases of coherent structures significantly contribute to the exchange of energy and matter throughout the entire volume of the roughness sublayer.

The probability density functions (pdf) of selected parameters for each of the exchange regimes are given in Fig. 4. The atmospheric stability parameter $\zeta = (z\text{–}d)\, L^{-1}$, where z is the height of the uppermost measurement level [m], d is displacement height [m] and L is Obukhov-length [m], shows a transition from rather stable to unstable conditions with increasing volume that participates in the mixing. The two exchange regimes W and C contain only stable and unstable data, respectively, whereas the regimes representing partly coupled states peak at neutral stratification. The pdfs of the friction velocity do not significantly differ amongst regimes with dominating turbulence (Dc, Ds, Cs and C), whereas the occurrence of wave motion is connected to smaller friction velocities as expected. From this follows that the friction velocity measured above the canopy may not serve as a reliable indicator for the coupling between the atmosphere, the canopy and the air close to the ground surface. The vertical gradient of the longitudinal wind speed shows very little variation amongst the exchange regimes with a consistent mean value of approximately $0.2\ m\ s^{-1}\ m^{-1}$.

For the footprint modelling, the decoupling of parts of the canopy space from the atmosphere was exclusively represented by the employed turbulence statistics. The LS model itself was not modified to simulate these cases, e.g., by introduction of a reflecting height at the canopy top for wave motion cases. In this context, decoupling does not describe an impermeable barrier blocking all particle motions, but a region of extremely weak

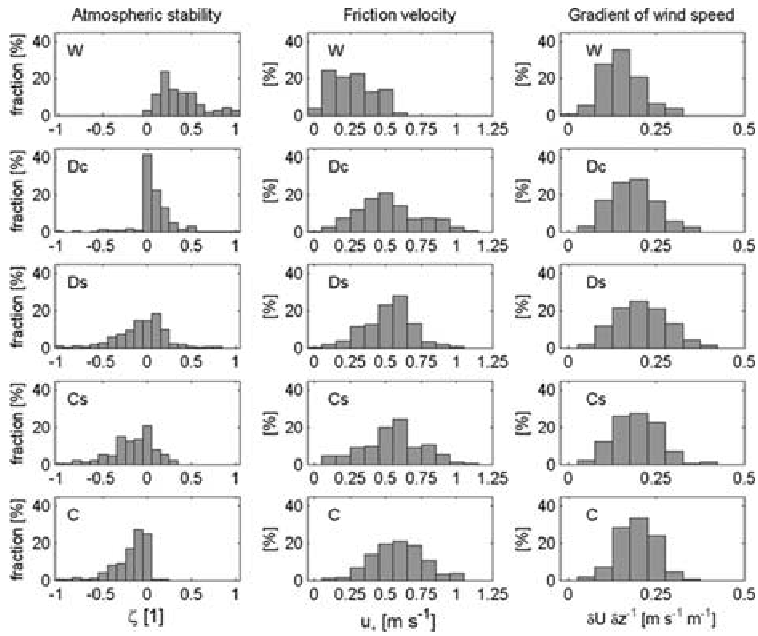

Fig. 4. Probability density functions of half-hourly averages of the atmospheric stability parameter ζ = (z–d) L^{-1} at 33 m, friction velocity u_* at 33 m, and vertical gradient of the longitudinal wind speed dU/dz at the canopy top for the five different exchange regimes: Total numbers of 30-min assigned periods were 134 (W), 271 (Dc), 310 (Ds), 131 (Cs) and 200 (C). The measurement period was June 24 to July 17.

turbulence that traps the particles, and eventually releases them into the atmosphere only after considerable horizontal transport in downwind direction.

5. Results

5.1. Conditionally-averaged profile measurements of velocity statistics for different exchange regimes

One averaging interval of 30-min length for each of the five exchange regimes was chosen to describe the turbulent flow field (Fig. 5). It should be noted that these individual, but representative sample cases will be replaced by the mean statistics for each exchange regime in a later project stage; however, the use of individual profiles could introduce additional bias into the results at this stage of the project. The stability parameters ζ = z/L for each exchange regime is given in the figure caption.

For the wave motion (W) regime, high absolute values and a strong gradient of the normalized wind speed are observed above the canopy. The normalized vertical momentum flux has a relatively large gradient in this region, whereas low absolute values are found close to and within the canopy. Standard variations of the wind components are rather low, except of the crosswind component, which shows a strong gradient above the canopy.

For Dc cases, the highest variation is found amongst the profiles shown in Fig. 5. The strong gradient of the normalized horizontal wind speed close to the canopy top is associated with a strong gradient of the vertical momentum flux at this level. This results in very high absolute values of the shear stress above the canopy (see Fig. 5b), while within the canopy the profile quickly drops to a level close to zero. The standard deviations of the wind components follow the same pattern showing the strongest gradients close to the canopy top, with a particularly large increase for the alongwind component.

The exchange regimes decoupled subcanopy (Ds) and Cs show similar patterns in the measured profiles, even though absolute values differ. For both these regimes, turbulence is more developed in the canopy space compared to the Dc regime, so that the strongest gradients are found where the LAI maximum is located (≈0.75 h_c). This particularly applies for the vertical momentum flux, with high absolute values in the upper canopy space, and low turbulence with decreasing height. In general, except for the trunk space region, both the average gradients in the canopy space and the absolute values of the profile data are larger for the Ds regime than those for the Cs regime; however, the latter observation may only be representative for the sample profiles chosen for this study.

For the fully coupled canopy (C), a pronounced local maximum (in absolute values) of the vertical momentum flux was observed. According to the high abundance of cases with unstable stratification and the corresponding intensive turbulent mixing, the normalized standard deviations of the wind components are generally higher than for any other exchange regime. As expected, only for the C regime can significant turbulent mixing be observed down into the subcanopy space.

5.2. Footprint results for different exchange regimes

The footprint model runs require continuous profiles for all input parameters up to the top of the model domain. Thus, data have to be interpolated between the measurement levels, and profiles must be extended to the ground level and into the atmospheric surface layer (ASL). After testing several options of profile interpolation, for the remaining study we chose linearly interpolated

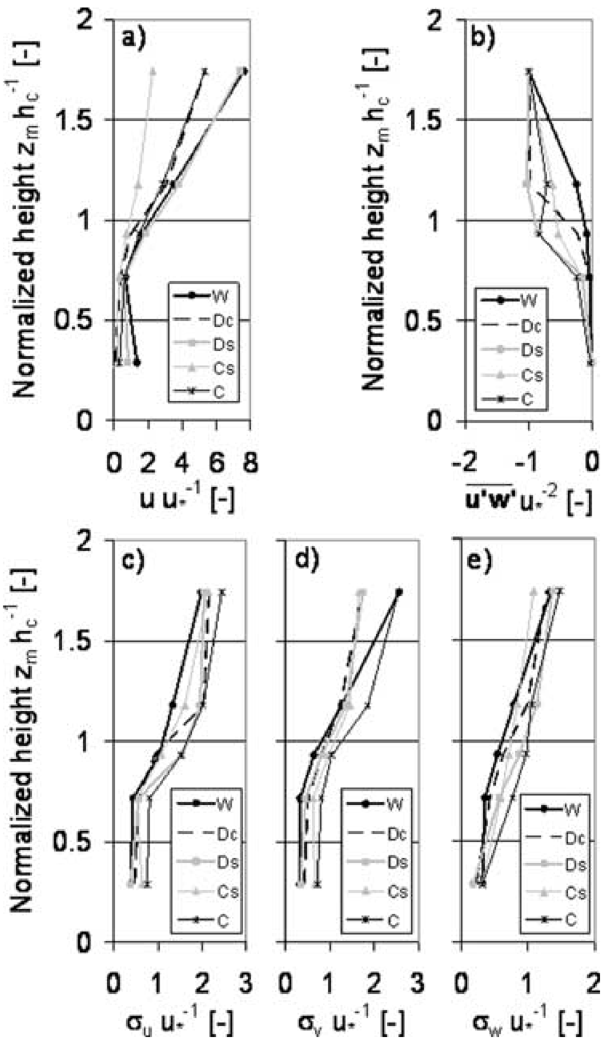

Fig. 5. Representative profiles of measured turbulence statistics for the five exchange regimes: wind speed (a), vertical momentum flux (b), standard deviation of alongwind (c), crosswind (d) and vertical wind (e). Values normalized with friction velocity. The measurement period was June 24 to July 17. The stability parameter ζ at the uppermost profile level ranges from very stable (W, $\zeta = 0.534$) over stable (Ds, $\zeta = 0.101$) and near-neutral (Dc, $\zeta = 0.015$) to unstable (Cs, C, $\zeta = -0.286$).

profiles. Above the highest measurement level, a constant gradient was applied up to a height of 2 h_c, which roughly represents the upper RSL (e.g. Garratt, 1980; Leuning, 2000; Arya, 2001), to linearly couple measured profiles to ASL profiles parametrized using Monin–Obukhov similarity functions as given in Rannik et al. (2003). Below the lowest measurement level, values were kept constant down to the surface.

Three sets of LS footprints were calculated for all five exchange regimes specified above (Fig. 6): The first based on WALDATEM measurement data (Fig. 5), the second with profiles of turbulence statistics modelled with the approach by Massman and Weil (1999) and the third using the profiles of Rannik et al. (2003); the latter two are shown in Fig. 2. The latter two have been included here to show the effect of using sources of velocity statistics that are easily available, but cannot describe the local conditions as accurately as measurements.

In Fig. 6, footprint differences between the exchange regimes are largely influenced by differences in atmospheric stability. The stability parameter ζ ranges from very stable (W, $\zeta = 0.534$) over stable (Ds, $\zeta = 0.101$) and near-neutral (Dc, $\zeta = 0.015$) to unstable (Cs, C, $\zeta = -0.286$), according to measurements at the uppermost profile level. As Monin–Obukhov theory was used for extrapolation purposes in the atmospheric boundary layer (see Rannik et al., 2003), atmospheric stability has a dominant impact on the shape of the modelled profiles.

The differences between the footprints computed from the measured WALDATEM profiles and the two references decrease with increasing coupling of the canopy space to the ASL. We observed significant deviations for the wave motion regime (W) concerning both position and height of the footprint peak. For the Dc case, the footprint functions differ mainly in the more pronounced peak derived with the measured profiles, which causes the cumulative footprint function to reach the maximum level at a much closer distance to the tower. For the Ds, the peak of the footprints based on measured profiles is shifted in upwind direction. However, looking at the cumulative footprint function, this shift is balanced further upwind as the footprint based on modelled profiles drops more quickly to a lower level. For the regimes with Cs and C, the differences between the three footprint functions are small.

6. Discussion

The results presented in the preceding section emphasize that the use of locally measured profiles of the turbulence statistics as input for an LS footprint model may have significant influence on the computed source areas. Moreover, for the five different coupling regimes between ground surface, canopy and atmosphere as determined by spectral wavelet analysis, individual characteristics of the flow statistics within and above the canopy were found to impact the shape and position of the computed source areas in many ways. This suggests that it may not be sufficient to run a footprint analysis for a given site with only a single set of flow statistics to describe the model domain; however, the compatibility of the specified conditions of turbulent exchange with the requirements to operate an LS footprint model needs to be discussed in more detail.

The wave motion (W) profiles are possibly not truly representative for the transport processes, as for most W-cases the flow will not be stationary as assumed for the footprint modelling. During occurring wave motion, vertical scalar transport is almost absent and the flow statistics do not represent developed turbulence. This is particularly true for the parts of the profile within the subcanopy domain. The resulting extended

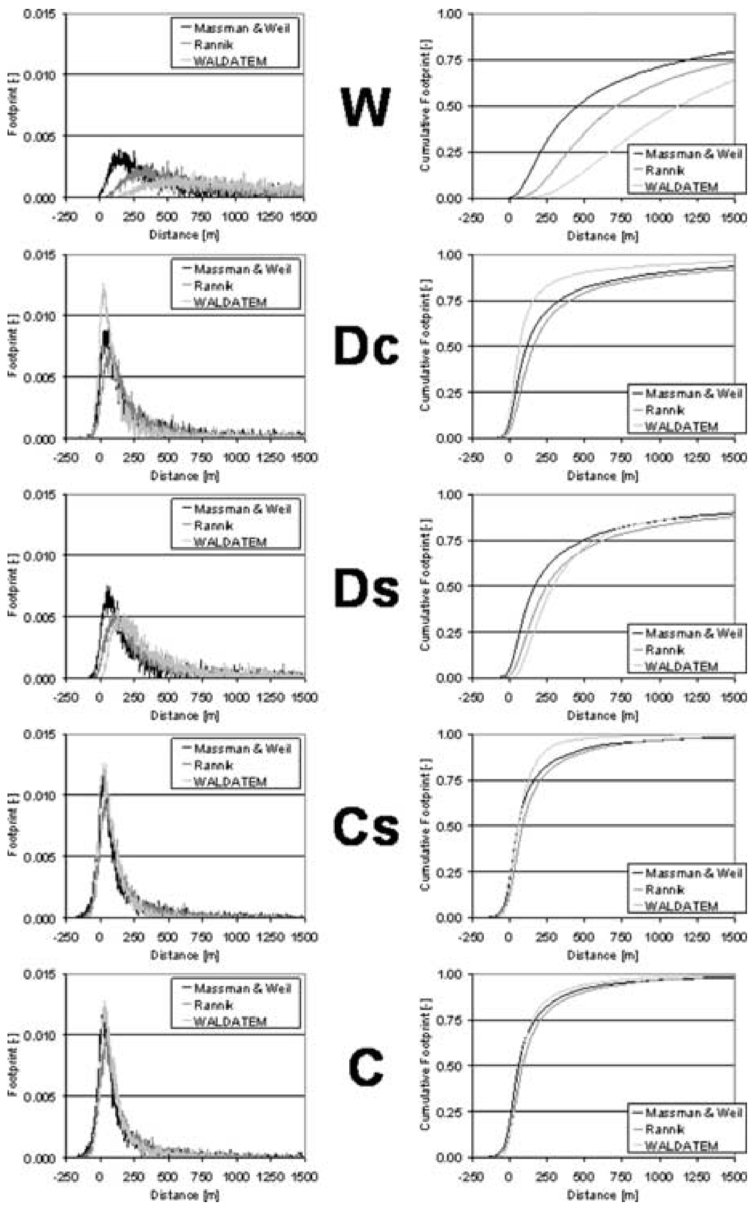

Fig. 6. Footprints calculated with the forward LS trajectory model based on measured WALDATEM data (light grey), profiles parametrized with the Massman & Weil model (black) and taken from Rannik et al. (2003, dark grey). Panels on the left show original crosswind integrated source weight functions, panels on the right give the accumulated footprints, both for the five different exchange regimes.

footprints are mainly due to high stability assigned to this exchange regime. The comparison between the footprints based on WALDATEM and reference profiles, respectively, indicate that the reference turbulence statistics overestimate the effectiveness in carrying the signal upwards toward the measurement level, as the peak position is closer to the measurement point in these cases. These findings suggest that footprint calculations for this exchange regime are unreliable, as neither measured nor modelled turbulence statistics describe the conditions in the upwind region in an adequate way for footprint modelling.

The exchange regimes of Dc and Ds can be discussed as a pair. For both regimes, the profiles of turbulence statistics are split in two sections, a well-mixed upper part and a decoupled lower part. In the case of a particle release height at 0.9 times the canopy height, which reduces the influence of the lower canopy on the model runs significantly, the results for both regimes are fairly similar. The most significant difference found for this release height is that the WALDATEM profiles produce more pronounced peaks than the references, indicating an underestimation of vertical transport in the modelled profiles.

Release of particles from the forest floor, however, reveals considerable differences between the Dc and the Ds regime. In the case of a Dc, the results are similar to the case with sources in the upper canopy, with the WALDATEM profiles causing a more pronounced peak than the modelled profiles. This may be caused by a reduced horizontal mobility of the particles due to low turbulence levels in the canopy space, so that the trajectories are still close to the source location when leaving the canopy. However, also the vertical turbulence is weak, which may balance the weak horizontal transport, so that further analyses are required here. In addition, further investigation is needed to see if this description adequately represents the exchange processes, or if the Dc is rather subject to intermittent ejections of sweeps to exchange particles with the ASL.

Conversely, in the Ds regime the WALDATEM profiles produce only slightly different footprints compared to the turbulence statistics of Rannik et al. (2003), whereas obvious differences in the peak location of the footprints were found for the parametrized profiles by Massman and Weil (1999). As shown in Fig. 6, the WALDATEM footprints peak approximately 100 m further upwind than those based on the modelled profiles. As the transport of the particles in the trunk space is based on very similar turbulence statistics for both the Dc and the Ds regime, this indicates a very effective horizontal transport within the upper part of the canopy. This interpretation is supported by the fact that for the Ds regime, strong gradients of normalized wind speed, standard deviation of the alongwind component and vertical momentum flux were observed (see Fig. 5).

Both examples for deviations between footprints based on measured or modelled turbulence statistics indicate that locally measured profiles are especially useful in case a part of the vertical model domain is decoupled from the ASL. In this case, very strong gradients or even local maxima or minima of the parameters describing the turbulent flow field frequently occur, which cannot be reproduced by modelling approaches. Furthermore, these characteristics of the profile data may influence the footprint calculations significantly, so that the use of a single modelled profile as input for LS footprint models will increase uncertainties especially in Dc or Ds situations.

Footprint results for all three sources of input data are fairly similar for the exchange regimes Cs and C, with the Cs regime peaking closer to the observation point than the C regime. This finding suggests that for convective turbulence, boundary layer processes often dominate over canopy layer effects (see also further below), so that the use of modelled turbulence statistics produces results which are close to those based on measurements, as long as there are no strong gradients within the profiles, and all areas are well-mixed due to a sufficient level of turbulence intensity throughout the canopy space.

The interpretation of the influence of the specific profile characteristics for different exchange regimes is compromised by the fact that they represent different stabilities, which also significantly influence the shape and position of the footprint. A direct comparison is only possible between the cases Cs and C, which both have a stability parameter $\zeta = -0.286$ at the highest measurement level. Differences are only small between the model runs based on WALDATEM profiles and parametrized turbulence statistics; however, the influence of the different turbulence statistics can clearly be seen in the cumulative footprint functions. For the measured profiles, the 90%-footprint has an extension of only ≈230 m for the Cs regime, while for the C regime this distance is ≈340 m, thus the footprint is ≈50% larger. In both cases, the 90% footprint based on the Massman and Weil (1999) profiles has a maximum distance of ≈420 m from the tower.

The role of atmospheric stability also has to be considered for the results about the impact of locally measured profiles of velocity statistics during different exchange regimes. For the C-regimes, which are mostly convective, vertical fluxes are often dominated by large eddies, which mix the entire boundary layer, including the canopy. As all three approaches to generate profiles for footprint modelling used the same boundary layer profiles, only insignificant differences between surface energy fluxes and footprints were found under these conditions. Differences amongst the three approaches showed up with increasing atmospheric stability. So for the W regime, which is found mostly for stable cases, even small details in the profiles may have a large impact on the exchange processes, and consequently there are significant differences in the footprint prediction.

Concerning the footprints computed with the profiles published by Rannik et al. (2003), our results demonstrate the value of a description of the turbulent flow field that has been adapted to the local conditions. The Rannik data are well adapted to their Northern Scots pine forest, but due to a different canopy architecture they are not truly representative for the spruce forest at the Waldstein Weidenbrunnen site. This is emphasized by the differences between the footprints based on the Rannik et al. (2003) measurements and those parametrized with the model by Massman and Weil (1999). However, also in this case the interpretation has to consider atmospheric stability, as the Rannik footprints still allow a very good footprint prediction for unstable cases often dominated by boundary layer processes, while the differences increased with an increasing stability parameter.

In this study, we did not consider possible turning of the mean wind direction as the flow penetrates into the canopy space. This may have considerable influence on the dispersion especially under low wind speeds above the canopy, and will be addressed by using a more advanced footprint algorithm in subsequent studies. Furthermore, the LS dispersion model by Thomson (1987) assumes Gaussian turbulence and thus cannot take into account the skewness of turbulence neither inside the canopy and trunk space nor above the canopy within the convective boundary layer (CBL). As the degree of skewness varies among different flow regimes, this may bias the results.

7. Summary

The comparison of footprints based on profiles measured in-situ with those based on reference profiles revealed significant differences in both the form and the position of the source weight functions. These differences could be linked to different exchange regimes, indicating that it may not be sufficient to run a footprint analysis with just a single set of profiles.

Concerning the effect of the exchange regime on the footprint calculations, results can be organized in three groups. First, in the case of W, footprint calculations are generally unreliable, as turbulence is not the dominating mode of the flow, and cannot be expected to be stationary as required for footprint modelling. Second, for exchange regimes with the lower section of the profiles decoupled from the ASL (Dc, Ds), significant differences between footprints based on measured or modelled profiles were observed. These can be attributed to profile characteristics, such as strong gradients or local maxima or minima, which cannot be reproduced by the modelling approaches. As a decoupling of the lower profile sections was observed for more the 50% of the WALDATEM-2003 data set analyzed in this study, we conclude that conditions as such are likely to be important for sites with tall canopies of moderate density. From this follows that profiles of the flow statistics considering this effect are expected to improve the accuracy of LS footprint modelling significantly. Third, for exchange regimes which at least partly couple the full canopy space to the atmospheric surface layer (Cs, C), well-mixed conditions are observed throughout the canopy space, and footprints based on the reference profiles were very similar to those based on the measured flow statistics.

Future work on this project will include the derivation of mean profiles of flow statistics for each exchange regime. It will also analyze how atmospheric stability influences the profiles, and discuss the turbulent field in the spatial context of the experimental site, where conditions vary with wind direction. In footprint modelling, three-dimensional footprints will be calculated to assess the effect of the locally measured profiles on the composition of land cover types within the source weight function. In addition, we will use the improved profiles in an advanced version of the LS footprint model, which allows for changing wind directions within the canopy space.

8. Acknowledgments

We acknowledge the contributions of Teresa Bertolini (Dept. Scienze Ambientali, Univ. Naples, Italy), Johannes Lüers, Johannes Olesch (both Dept. Micrometeorology, Univ. Bayreuth, Germany), Jens-Christopher Mayer (now Max-Planck Institute for Chemistry, Mainz, Germany) and Joel Schröter (now Meteorology and Air Quality Section, Univ. Wageningen, The Netherlands) in the WALDATEM-2003 experiment. This research was supported by the Office of Science (BER), U.S. Department of Energy, Grant No. DE-FG02-04ER63911 (AmeriFlux Measurement Network: Science Team Research), the German Federal Ministry for Education and Research (BMBF), DFG Fo 226/10-1 and the Academy of Finland (project No. 109601).

References

Antonia, R. A., Browne, L. W. B., Bisset, D. K. and Fulachier, L. 1987. A description of the organized motion in the turbulent far wake of a cylinder at low Reynolds numbers. *J. Fluid. Mech.* **184**, 423–444.

Arya, S. P. 2001. Introduction to Micrometeorology. Academic Press, San Diego, pp. 415.

Aubinet, M., Grelle, A., Ibrom, A., Rannik, Ü., Moncrieff, J. and co-authors. 2000. Estimates of the annual net carbon and water exchange of forests: The EUROFLUX methodology. *Adv. Ecol. Res.* **30**, 113–175.

Baldocchi, D. D. 1997. Flux footprints within and over forest canopies. *Bound.-Layer Meteorol.* **85**, 273–292.

Baldocchi, D. D., Finnigan, J. J., Wilson, K., Paw U., K. T. and co-authors. 2000. On measuring net ecosystem carbon exchange over tall vegetation on complex terrain. *Bound.-Layer Meteorol.* **96**, 257–291.

Baldocchi, D. D., Falge, E., Gu, L., Olson, R., Hollinger, D. and co-authors. 2001. FLUXNET: A new tool to study the temporal and spatial variability of ecosystem-scale carbon dioxide, water vapour and energy flux densities. *Bull. Amer. Meteorol. Soc.* **82**, 2415–2435.

Finnigan, J. J. 2000. Turbulence in Plant Canopies. *Annu. Rev. Fluid Mech.* **32**, 519–571.

Foken, T., Göckede, M., Mauder, M., Mahrt, L., Amiro, B. D. and co-authors. 2004. Post-field data quality control. In: *Handbook of Micrometeorology: A Guide for Surface Flux Measurements* (eds. X. Lee, W. J. Massman, and B. E. Law). Kluwer Academic Publishers, Dordrecht, pp. 181–208.

Garratt, J. R. 1980. Surface influence upon vertical profiles in the atmosphere near-surface layer. *Quart. J. Roy. Meteorol. Soc.* **106**, 803–819.

Gerstberger, P., Foken, T. and Kalbitz, K. 2004. The Lehstenbach and Steinkreuz catchments in NE Bavaria, Germany. In: *Biogeochemistry of Forested Catchments in a Changing Environment, Ecological Studies, Vol. 172* (ed. E. Matzner). Springer, Berlin, Heidelberg, New York, pp. 15–44.

Göckede, M., Rebmann, C. and Foken, T. 2004. A combination of quality assessment tools for eddy covariance measurements with footprint modelling for the characterisation of complex sites. *Agric. For. Meteorol.* **127**, 175–188.

Göckede, M., Markkanen, T., Hasager, C. B. and Foken, T. 2006. Update of a footprint-based approach for the characterisation of complex measurement sites. *Bound.-Layer Meteorol.* **118**, 635–655.

Horst, T. W. and Weil, J. C. 1992. Footprint estimation for scalar flux measurements in the atmospheric surface layer. *Bound.-Layer Meteorol.* **59**, 279–296.

Kljun, N., Rotach, M. W. and Schmid, H. P. 2002. A three-dimensional backward Lagrangian footprint model for a wide range of boundary-layer stratifications. *Bound.-Layer Meteorol.* **103**, 205–226.

Leclerc, M. Y. and Thurtell, G. W. 1990. Footprint prediction of scalar fluxes using a Markovian analysis. *Bound.-Layer Meteorol.* **52**, 247–258.

Lee, X. 1998. On micrometeorological observations of surface-air exchange over tall vegetation. *Agric. For. Meteorol.* **91**, 39–49.

Leuning, R. 2000. Estimation of scalar source/sink distributions in plant canopies using Lagrangian dispersion analysis: Corrections for atmospheric stability and comparison with a multilayer canopy model. *Bound.-Layer Meteorol.* **96**, 293–314.

Marcolla, B., Pitacco, A. and Cescatti, A. 2003. Canopy architecture and turbulence structure in a coniferous forest. *Bound.-Layer Meteorol.* **108**, 39–59.

Massman, W. J. 1997. An analytical one-dimensional model of momentum transfer by vegetation of arbitrary structure. *Bound.-Layer Meteorol.* **83**, 407–4021.

Massman, W. J. and Weil, J. C. 1999. An analytical one-dimensional second-order closure model of turbulence statistics and the Lagrangian time scale within and above plant canopies of arbitrary structure. *Bound.-Layer Meteorol.* **91**, 81–107.

Rannik, Ü., Markkanen, T., Raittila, J., Hari, P. and Vesala, T. 2003. Turbulence statistics inside and over forest: Influence on footprint prediction. *Bound.-Layer Meteorol.* **109**, 163–189.

Rannik, Ü., Aubinet, M., Kurbanmuradov, O., Sabelfeld, K. K., Markkanen, T. and Vesala, T. 2000. Footprint analysis for measurements over a heterogeneous forest. *Bound.-Layer Meteorol.* **97**, 137–166.

Rebmann, C., Göckede, M., Foken, T., Aubinet, M., Aurela, M. and co-authors. 2005. Quality analysis applied on eddy covariance measurements at complex forest sites using footprint modelling. *Theor. Appl. Climatol.* **80**, 121–141.

Sawford, B. L. 1985. Lagrangian stochastic simulation of concentration mean and fluctuation fields. *J. Clim. Appl. Meteorol.* **24**, 1152–1166.

Schmid, H. P. 1997. Experimental design for flux measurements: matching scales of observations and fluxes. *Agric. For. Meteorol.* **87**, 179–200.

Schmid, H. P. 2002. Footprint modelling for vegetation atmosphere exchange studies: a review and perspective. *Agric. For. Meteorol.* **113**, 159–183.

Schmid, H. P. and Oke, T. R. 1988. Estimating the source area of a turbulent flux measurement over a patchy surface. In: *Proceedings of the 8th Symposium on Turbulence and Diffusion*, American Meteorological Society, Boston, MA, pp. 123–126.

Schuepp, P. H., Leclerc, M. Y., MacPherson, J. I. and Desjardins, R. L. 1990. Footprint prediction of scalar fluxes from analytical solutions of the diffusion equation. *Bound.-Layer Meteorol.* **50**, 355–373.

Thomas, C. and Foken, T. 2005. Detection of long-term coherent exchange over Spruce Forest using wavelet analysis. *Theor. Appl. Climatol.* **80**, 91–104.

Thomas, C. and Foken, T. 2006. Organised motion in a tall spruce canopy: temporal scales, structure spacing and terrain effects. *Bound.-Layer Meteorol.*, DOI 10.1007/s10546-006-9087-z.

Thomas, C. and Foken, T. 2007. Flux contribution of coherent structures and its implications for the exchange of energy and matter in a tall spruce canopy. *Bound.-Layer Meteorol.*, DOI 10.1007/s10546-006-9144-7.

Thomas, C., Ruppert, J., Lüers, J., Schröter, J., Mayer, J. C. and co-authors. 2004. *Documentation of the WALDATEM-2003 Experiment*. Universität Bayreuth, Abteilung Mikrometeorologie, Arbeitsergebnisse, Print ISSN 1614-8916, pp. 59.

Thomson, D. J. 1987. Criteria for the selection of stochastic models of particle trajectories in turbulent flows. *J. Fluid Mech.* **180**, 529–556.

Wilson, J. D. and Sawford, B. L. 1996. Review of Lagrangian stochastic models for trajectories in the turbulent atmosphere. *Bound.-Layer Meteorol.* **78**, 191–210.

Wilson, J. D., Legg, B. J. and Thomson, D. J. 1983. Calculation of particle trajectories in the presence of a gradient in turbulent-velocity variance. *Bound.-Layer Meteorol.* **27**, 163–169.